ELECTRON TECHNOLOGY
ISSN 1897-2381
http://www.ite.waw.pl/etij/
Internet Journal

QUANTUM POINT CONTACT SIMULATIONS ON ISIS STRUCTURE

G. HAŁDAŚ, M. MĄCZKA

Rzeszów University of Technology, ul. W. Pola 2, 35-959 Rzeszów, Poland

Received Dec. 7, 2006; accepted Dec. 12, 2006; published Dec. 19, 2006

ABSTRACT

In the work a numerical method of dissolving the Poisson equation in an electrostatically formed Quantum Point Contact (QPC) is described. Such a device is based on the structure called ISIS (Inverted Semiconductor Insulator Semiconductor). This structure was proposed in 1991 by Kastner [1] who made single electron transistor in it. In this paper the Poisson equation is solved by means of boundary elements method [2] with functions of the single layer potential [3] whose result provides potential distributions of the QPC device. The electronic properties of the QPC model are found by the use of Green functions method [4]. The interaction between structure and two leads is described by self-energy method [5]. The QPC conductance is calculated with the help of Landauer formula, after the Green's function corresponding to device Hamiltonian is evaluated.

1. Introduction

In the paper we present the simulation method of quantum point contact (QPC) based on the inverted semiconductor insulator semiconductor (ISIS) structure. This device was introduced in 1991 by Kastner [1] et al. We start our analysis using the same type of the structure. In order to create the model of quantum point contact (Fig. 1) we deposit suitably formed metal electrodes on the surface. A suitable biasing of electrodes forms two-dimensional electron gas (2DEG) on the interface between top layer i-GaAs and the i-AlGasAs layer. Its density is controlled by the gate voltage applied to the lower (G) electrode deposited on conductive substrate. A negative voltage applied to the upper electrodes (E) depletes 2DEG underneath them. The electrostatic potential takes the form of saddle in the region where the gas is constricted.

When the voltage applied to (E) electrodes is decreased, the potential constriction and open channels are reduced. The conductance of such device is proportional to the number of open channels therefore we observe *plateaus* equaled $n\times 2e^2/h$, where n is number open channels.

2. Numerical model and simulation method

The model of examination of the quantum point contact is shown in Fig. 1. The model consists of five regions with fixed potentials corresponding to metallic electrodes: lower gate (G), source (S), drain (D) and suitably formed metal electrodes (E) on the surface. The process of simulations consists of two steps.

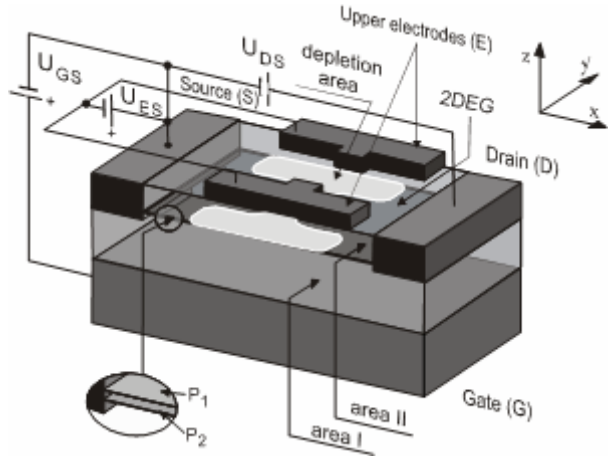

Fig. 1. Model of quantum point contact.

2.1. Calculation of potential distribution in QPC

The first step relies on solution of Poisson equation:

$$\Delta\varphi = -\frac{\rho}{\varepsilon}, \qquad (1)$$

where ρ is volume density of electric charge (in the considered case it is an unbalanced charge in the 2DEG area) with boundary conditions described by

a potential fixed on the electrode and the 2DEG area. The conditions of continuity of potential and normal component of the vector of electric displacement field on surface which differentiates area *I* and *II* are as fallows:

$$\begin{aligned} \varphi_i\big|_{S_k} &= V_k \qquad i = 1,2 \\ \varphi_1\big|_{P_1} &= \varphi_2\big|_{P_2} \qquad , \\ \varepsilon_1 \frac{\partial \varphi_1}{\partial z}\bigg|_{P_1} &= \varepsilon_2 \frac{\partial \varphi_2}{\partial z}\bigg|_{P_2} \end{aligned} \tag{2}$$

where S_k is the surface of the k-th electrode; indices 1, 2 are concerned with the potentials in areas *I* and *II,* respectively, and V_k denotes potential of k-th electrode. Because ρ is unknown, the solution of our task has to lead to necessary self-consistency ρ and φ fields.

In the first step $\rho = 0$ is accepted therefore Laplace equation is solved for the above-mentioned boundary conditions.

The function φ has to be found in form of the single layer potential:

$$\varphi_i(p_i) = \frac{1}{4\pi\varepsilon_i} \int_{S_i} \frac{\sigma_{S_i}}{r} ds_i , \qquad i = 1,2 , \tag{3}$$

where σ_S is the potential density of the single layer on a S_i surface which is the boundary of the i-th area. In this equation r is the distance of point p_i of this area to any other any point on the boundary.

Substituting Eq. (3) to the boundary conditions, the matrix of integral equations is found, with unknown σ_S. Once a set of integral equations is solved, a desired function of the potential is obtained according to Eq. (3).

To solve the problem, which was mentioned above, the Boundary Elements Method is used. On the electrodes as well as on the surfaces P_1, P_2 a rectangular mesh, with the elements of different sizes is defined. This makes the compromise between the accuracy of the calculations and size of numerical model, limited by a memory size of the computer.

The functions of potential densities, are approximated by the elements of a discretization mesh and by staircase functions, therefore expression (3) has the following form:

$$\varphi_P = \frac{1}{4\pi\varepsilon_i} \sum_{n=1}^{N_i} \sigma_{S_{in}} \iint_{S_{in}} \frac{ds_i}{r} \quad \text{dla} \quad P \in S_i , \tag{4}$$

where S_{in} denotes the area of the n-th element of the discretization mesh on surface of the boundary of the area S_i.

After the substitution of Eq. (4) to boundary conditions (2) the system of algebraic Eqs. (5) of a σ_S variables is obtained. Integrals in Eq. (4) are calculated analytically. In the system of Eqs. (5) N_1 and N_2 are the numbers of the discretization elements on the boundary of 1 and 2 areas, respectively (see Fig. 1),

$$\begin{cases} \dfrac{1}{4\pi\varepsilon_1} \displaystyle\sum_{n=1}^{N_1} \sigma_{S_{1,n}} \iint_{S_{1,n}} \frac{ds_{1,n}}{r_{n,m}} = V_{S_1,m} & m = 1 \ldots N_1 \\ \dfrac{1}{4\pi\varepsilon_2} \displaystyle\sum_{n=1}^{N_2} \sigma_{S_{2,n}} \iint_{S_{2,n}} \frac{ds_{2,n}}{r_{n,m}} = V_{S_2,m} - V_{2DEGm} & m = 1 \ldots N_2 \\ \dfrac{1}{\varepsilon_1} \displaystyle\sum_{n=1}^{N_1} \sigma_{S_{1,n}} \iint_{S_{1,n}} \frac{ds_{1,n}}{r_{n,k}} = \frac{1}{\varepsilon_2} \sum_{n=1}^{N_2} \sigma_{S_{2,n}} \iint_{S_{2,n}} \frac{ds_{2,n}}{r_{n,k}} & m = 1 \ldots N_3 \\ \varepsilon_1 \displaystyle\sum_{n=1}^{N_1} \sigma_{S_{1,n}} \iint_{S_{1,n}} \frac{\partial}{\partial z} \frac{1}{r_{n,k}} ds_{1,n} = \varepsilon_2 \sum_{n=1}^{N_2} \sigma_{S_{2,n}} \iint_{S_{2,n}} \frac{\partial}{\partial z} \frac{1}{r_{n,k}} ds_{2,n} & m = 1 \ldots N_3 \end{cases} \tag{5}$$

N_3 is the number of the discretization elements on P_1 and P_2 surfaces (see inset Fig. 1), $V_{S_i,m}$ is the fixed potential on a surface of the m-th element on the boundary of the i-th area and V_{2DEG} is the induced potential from the 2DEG area (in first iteration V_{2DEG}=0). One unknown variable in (5) is σ_S. The matrix of coefficients of the set of Eqs. (5) is solved by means of the Gauss elimination method.

The next step of calculations relies on matching a charge in the 2DEG and the electrodes.

2.1.2. Two-dimensional electron gas

The value of the charge in quantum point contact and the 2DEG area is calculated on the basis of the formula which defines a concentration of the two-dimensional electron gas [6]:

$$n_{2DEG} = \frac{m}{\pi\hbar^2} \int_{E_C}^{\infty} f(E, E_F) dE = \frac{m k_B T}{\pi\hbar^2} \ln\left(1 + \frac{E_F}{k_B T}\right), \tag{6}$$

where f is the function of Fermi-Dirac distribution, E_F is Fermi energy of the 2DEG, E_C is energy of the bottom edge of the conductivity subband, m is an effective mass of electron. The formula (6) is valid in the case of sufficiently large quantum point contacts, i.e. the ones that include statistically significant number of electrons [6].

In order to calculate parameters of the 2DEG we analyzed the conduction band in region of hetero-juncion in our model of device. For positive U_{GS}, triangular well is created in GaAs layer what is shown in Fig. 2.

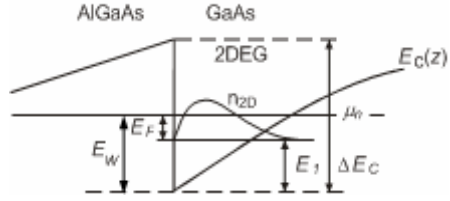

Fig. 2. The part of the conduction band $E_C(z)$ in the region of heterojunction AlGaAs-GaAs for U_{GS}>0.

According to Fig. 2 we can write:

$$E_W = E_1 + E_F , \tag{7}$$

where E_W is energy difference between Fermi energy

(μ_n) upper (E) electrode and energy of bottom of the well, E_1 is the lowest energy level. In order to solve the lowest energy level we use the triangular well approximation [6]:

$$E_1 = c_1 \left[\frac{\hbar^2}{2m} \left(\frac{e^2 n_{2DEG}}{\varepsilon_0 \varepsilon_r} \right)^2 \right]^{\frac{1}{3}}, \qquad (8)$$

where $c_1 \approx 2.338$. If the depth of the well is known, expressions (6), (7) and (8) may be transformed to obtain non-linear equation with only one unknown variable. We use it to find the Fermi energy (EF) of the 2DEG. Then the concentration of the 2DEG from Eq. (6) can be calculated.

Now the charge of the 2DEG can be computed. Substituting it to Eq. (1) and Eq. (3) to boundary conditions (2) we solve the set of Eqs. (5) including the induced potential from the 2DEG. The procedure is repeated until the electron density in electrodes and the 2DEG stops changing. Now it is possible to count the potential in any point P lying inside studied device in accordance to Eq. (4).

The study of potential energy distribution is concentrated close to AlGaAs-GaAs junction where the 2DEG is formed. At the end of the first step of calculation we obtain self-consistently of the potential energy distribution in the 2DEG area.

2.2. Conductance of QPC

The second step relies on the calculation of the conductance. In this step we take into account only the 2DEG area. Therefore the computations reduce to two-dimensional case. It is also assumed that QPC conductance is calculated for $U_{DS} \to 0$ (source-drain voltage), and the temperature is close to 0K. Then the conductance g between contacts 1 (drain) and 2 (source) is given by summing up the transmission probabilities T_{mn} between each pair of modes, namely mode m in lead 2 and mode n in lead 1

$$g = \frac{2e^2}{h} \sum_{m \in L_2} \sum_{n \in L_1} T_{mn} \qquad (9)$$

This is well-known Landauer formula [7]. The transmission probabilities T_{mn} are directly connected to the elements of S-matrix, relating the electron wave function amplitudes in different leads: $T_{mn} = |s_{mn}|^2 v_m / v_n$, where v_m, v_n are velocities in modes m and n, respectively. One way of calculating the S-matrix elements is to employ the Fisher-Lee relation which express T_{mn} in terms of the Green's function [8].

2.2.1. Green's function

The Green's function describes the response at any point $\mathbf{r}$ due to the excitation at point $\mathbf{r}'$. In general, when the response is related to the excitation by a differential operator H the Green's function $G(\mathbf{r}, \mathbf{r}', E)$ can be defined as the solutions of inhomogeneous differential equation [4]

$$(z - H) G(\mathbf{r}, \mathbf{r}', z) = \delta(\mathbf{r} - \mathbf{r}'), \qquad (10)$$

where z is complex variable with $E = \mathrm{Re}\{z\}$ and $\eta = \mathrm{Im}\{z\}$. When H is linear, time-independent Hermitian deferential operator which possesses the set of ortonormal eigenfunctions $\{\phi_n(\mathbf{r})\}$ corresponding to eigenvalues E_n:

$$H\phi_n(\mathbf{r}) = E_n \phi_n(\mathbf{r}), \qquad (11)$$

one can express $G(\mathbf{r}, \mathbf{r}', z)$ as eigenfunction expansion

$$G(\mathbf{r}, \mathbf{r}', z) = \sum_n \frac{\phi_n(\mathbf{r}) \phi_n^*(\mathbf{r}')}{z - E_n} + \int dn \frac{\phi_n(\mathbf{r}) \phi_n^*(\mathbf{r}')}{z - E_n}, \qquad (12)$$

where $\int dn$ is the integral over continuous spectrum (band) of H. The above equation shows that G has the poles at the positions of discrete eigenvalues E_n of the Hamiltonian. Since H is Hermitian its eigenvalues are real and thus the poles of G lie only on the real axis in complex z-plane. The residue at a pole E_n equals to $\Sigma_k \phi_k(\mathbf{r}) \phi_k^*(\mathbf{r})$ where the summation is over all degenerate eigenstates with eigenenergy E_n. The situation is quite different for energies belonging to the continuous spectrum of H consisting of extended states. In this case the Green's function is not well defined since the integrand in Eq. (4) has a pole. For such energies the retarded Green's function is defined by a limiting procedure

$$G^R(\mathbf{r}, \mathbf{r}', E) = \lim_{\eta \to 0^+} G(\mathbf{r}, \mathbf{r}', z). \qquad (13)$$

2.2.2. Tight Binding Hamiltonian

One of the most widely used models of electron device on the quantum mechanical level is the Tight Binding Hamiltonian (TBH). In this model the wave function is expressed in terms of localized atomic-like orbital (states), one at each atomic site. Usually it is assumed that only orbital on nearest neighboring (n.n.) sites overlap. The measure of this overlapping is the transfer integral t. If we assume that local potential influences the eigenenergy ε_i of electron located at site i then TBH in a braket notation has the form

$$H = \sum_i |i\rangle \varepsilon_i \langle i| - \sum_{i,j} |i\rangle t_{ij} \langle j| \qquad (14)$$

where $|i\rangle$ is the orbital centered at site i and the second sum runs only over n.n. The convenient way is to write H in a matrix representation:

$$\begin{aligned} [\mathrm{H}]_{ii} &= \varepsilon_i \\ [\mathrm{H}]_{ij} &= -t \quad \text{for } i, j \text{ being n.n.} \\ [\mathrm{H}]_{ij} &= 0 \quad \text{otherwise.} \end{aligned} \qquad (15)$$

In this case the differential equation of Eq.(10) becomes a matrix equation

$$(z[\mathrm{I}]-[\mathrm{H}])[\mathrm{G}]=[\mathrm{I}], \tag{16}$$

where [I] is the identity matrix and the Green's function becomes a matrix with elements

$$[\mathrm{G}]_{ij}=[\mathrm{G}]_{ij}(z)=G(\mathbf{r},\mathbf{r}',z) \tag{17}$$

which describes response at site i due to excitation in site j. Eq. (15) provides another way to calculate the Green's function

$$[\mathrm{G}]=(z[\mathrm{I}]-[\mathrm{H}])^{-1}. \tag{18}$$

The only problem is that the matrix is infinite dimensional. This is because of the leads, which should be considered as stretching out to infinity. Otherwise we would deal with closed system with no transport at all. The solution of this "infinite dimensional" problem is proposed in the book of Datta [5].

2.2.3. Self-energy

One obtains the formula for the Green's function of a device in which the interaction with the leads is taken into account:

$$[\mathrm{G}]=\left(z[\mathrm{I}]-[\mathrm{H_D}]-[\Sigma_{\mathrm{L1D}}]-[\Sigma_{\mathrm{L2D}}]\right)^{-1}, \tag{19}$$

where $[\mathrm{H_D}]$ is Hamiltonian matrix which describes the isolated device. The terms $[\Sigma_{\mathrm{L1D}}]$ and $[\Sigma_{\mathrm{L2D}}]$ that appear in Eq. (19) describe the interactions between the device and the lead 1, and the lead 2, respectively. They are called the self-energies (due to the leads). The self-energy matrix elements can be obtained from the equation [5], [9], [10]:

$$[\Sigma_{\mathrm{p}}]_{ij}(E)=-t\sum_m \chi_m(l_i)\chi_m(l_j)f_m(E), f_m(E)$$

$$=\begin{cases} q-\sqrt{q^2-1} & \text{for} \quad E\geq E_m+2t \\ e^{ik_m a} & \text{for} \quad |E-E_m|\leq 2t \\ q+\sqrt{q^2-1} & \text{for} \quad E\leq E_m-2t \end{cases} \tag{20}$$

where E_m is energy m-th mode, χ_m is the transverse components of the wave functions in the lead, t is the hopping element ($t\equiv\hbar^2/2m^*a^2$, a – constant lattice, m^* is effective mass) and $q=\cos k_m a=(E-E_m)/2t$.

3. Results

In this section we present the results of simulation for two kinds of the QPC. The device structure parameters are schematically shown in Fig. 3.

The parameters can be sorted into three groups. The first group (Fig. 3a) defines longitudinal and vertical size of structure, drain, source and the upper (E) electrodes. The second group (Fig. 3b) characterizes dielectric layer parameter, and thickness of the semiconductor layers and electrodes. Third group is described by voltage parameters.

The voltages biasing the structure are marked in Fig. 1.

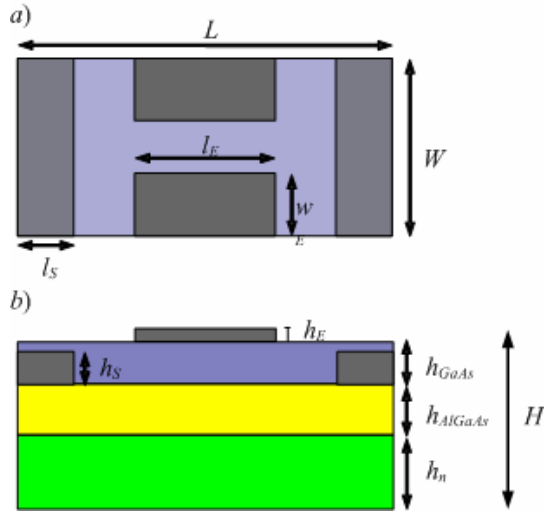

Fig. 3. The parameterization of the QPC model: a) view from the top of the structure, b) cross-section of the structure.

The values of basic parameters used in the simulation for the first sample of the QPC (QPC 1) are placed in Table 1, and for second sample (QPC 2) in Table 2. The value of biasing voltage U_{GS} is responsible for creating the 2DEG. In order to compare the models, this voltage is chosen so as to the concentration of gas near drain and source area has the same value. The concentration of the 2DEG approximates $2.5\cdot10^{15}$ m^{-2} for the biasing voltages equaled to 0.7 V and 0.4 V for the QPC 1 and the QPC 2, respectively.

Table 1. The values of the basic parameters of the simulations for the QPC 1

Sizes of the structure				Biasing voltages	
	[nm]		[nm]		[V]
L	600	H	620	U_{GS}	0.7
W	400	h_E	20	U_{ES}	–2.50÷–2.15
l_E	480	h_S	50	U_{DS}	0
l_S	100	h_{GaAs}	100	Dielectric permittivity	
w_S	20	h_{AlGaAs}	200	ε_1	12.8
		h_n	300	ε_2	13.2

Table 2. The values of the basic parameters of the simulations for the QPC 2

Sizes of the structure				Biasing voltages	
	[nm]		[nm]		[V]
L	700	H	520	U_{GS}	0.4
W	400	h_E	50	U_{ES}	–1.8÷–1.64
l_E	300	h_S	50	U_{DS}	0
l_S	100	h_{GaAs}	70	Dielectric permittivity	
w_S	50	h_{AlGaAs}	100	ε_1	12.8
		h_n	300	ε_2	13.2

As it was mentioned earlier, the calculation concentrated around AlGaAs interface. An example of the potential energy distribution in this area is shown in Fig. 4.

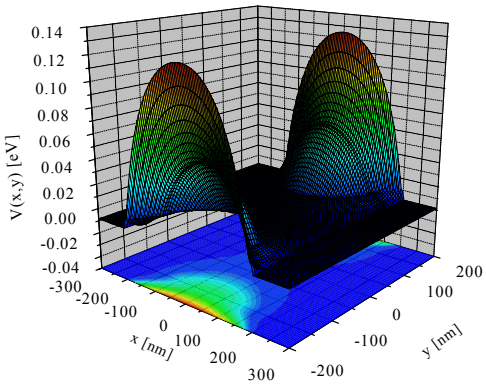

Fig. 4. The distribution of potential energy for QPC 1 in the 2DEG area calculated for $U_{GS} = 0.7$ V, $U_{ES} = -2.34$ V and $U_{DS} = 0$ V.

The potential energy distribution was calculated for biasing voltages: $U_{GS} = 0.7$ V, $U_{ES} = -2.34$ V and $U_{DS} = 0$ V for the model (QPC 1), whose simulation parameters are shown in Table 1. In Fig. 4 we see that the distribution of the potential energy looks like the saddle.

The energy $V(x,0)$ varies with longitudinal position x through the constriction, rising to a broad peak in the middle. The peak energy in the constriction under the Fermi energy (in Fig. 5, $E_F = 0$) depends on biasing voltage in upper (E) electrodes (U_{ES}). If biasing voltage U_{ES} increases the constriction grows as well. This effect is shown in Fig. 5.

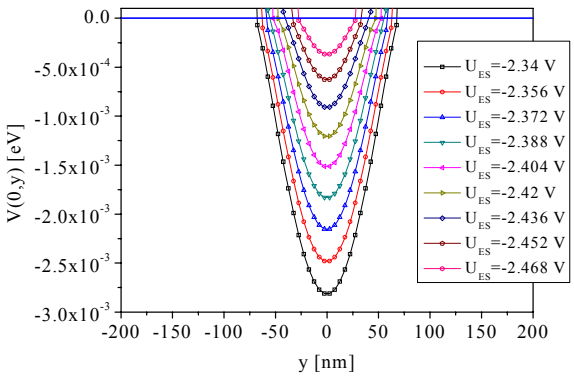

Fig. 5. The cross-section of the potential energy distribution through the centre of the model perpendicular to transport direction for various voltages U_{ES} for the QPC 1.

In Fig. 6 cross-sections of the potential energy distribution through the centre of the model along to transport direction for various voltages U_{ES} is presented.

In this case, if the biasing voltage U_{ES} is increased, the potential barrier is reduced. It enables the charge transport between source and drain. The electrons are forced to travel through the gap of constriction and behave like quasi-one-dimensional system.

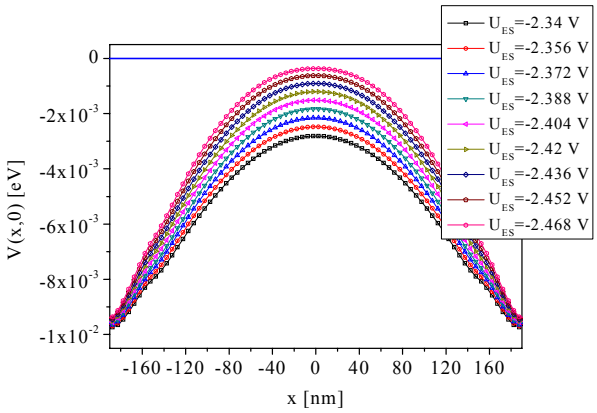

Fig. 6. The cross-section of the potential energy distribution through the centre of the model along with transport direction for various voltages U_{ES} for QPC 1.

In this system we observe the quantized conductance.

Figure 7 shows this effect for two models of the QPC in which staircases of conductance g versus the upper gate voltage U_{ES} are presented. U_{ES} is calculated from a sample-dependent threshold U_T. The threshold voltage depends on a geometry of the QPC. In our case it is equaled –2.48 V and –1.758 V for QPC 1 and QPC 2, respectively.

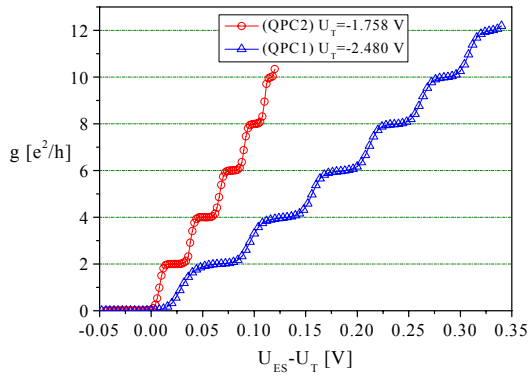

Fig. 7. The staircases of the conductance g versus the upper gate voltage U_{ES}, calculated form a sample-dependent threshold U_T.

For biasing voltages $U_{ES} > U_T$ we observe „staircase" increasing of the conductance and the conductance quant is equaled to $2e^2/h$, what is true according to the theory and experimental results [11], [12]. It is worth to notice that range of changes of conductance is lower for the QPC 2 then for the QPC 1.

The nature of changes of conductance depends on parameters of electrostatically formed potential. The transition of conductance from one *plateau* to next one is associated with the width of potential barrier in transport (x) direction. Figure 8 depicts that the barrier for the QPC 2 is wider then the QPC 1. The wider the barrier the more difficult tunneling throughout the barrier is observed. Only these

channels are on whose energy is greater or almost equal to the maximum energy of potential in the middle of constriction. For lesser barrier width (see

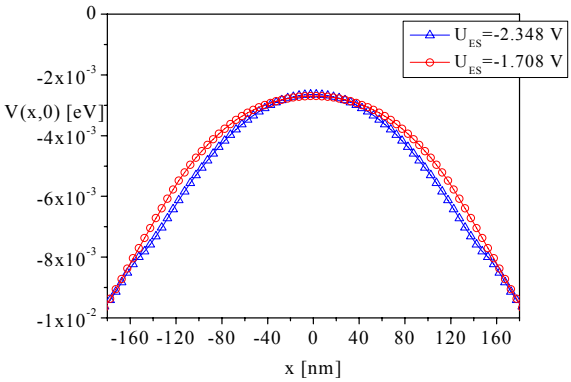

Fig. 8. The comparison of cross-sections of the potential energy distribution through the centre of the model along with transport direction calculated for (QPC 1) $U_{GS} = 0.7$ V, $U_{ES} = -2.348$ V and for (QPC 2) $U_{GS} = 0.4$ V, $U_{ES} = -1.708$ V.

Fig. 8) the increase of conductance is slow therefore the tunneling of electrons throughout the barrier is easier. Instead, the width of *plateaus* of conductance depends on steepness of the potential in perpendicular direction to the transport.

The greater the steepness the longer the *plateau*. Let us see, that the potential energy (Fig. 9) increases quicker for the QPC 2 then for the QPC 1, therefore a better visibility of the *plateau* in the characteristic is observed for QPC 2.

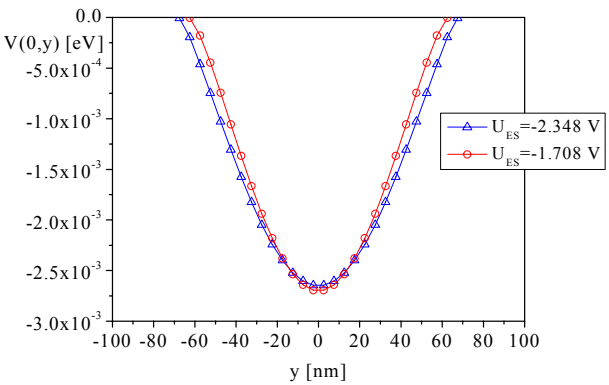

Fig. 9. The comparison of cross-sections of the potential energy distribution through the centre of the model perpendicular to transport direction calculated for (QPC 1) $U_{GS} = 0.7$ V, $U_{ES} = -2.348$ V and for (QPC 2) $U_{GS} = 0.4$ V, $U_{ES} = -1.708$ V.

4. Conclusions

The main goal of our work was to simulate and test numerical model of quantum point contact created using ISIS structure. On the basis of obtained results shown in Fig. 7 one is allowed to conclude that this goal was reached. Calculated conductance of proposed model is step-like what is a tipical feature of quantum point contact. An open subject is to discuss the quantitative changes of the range of switching the quantum mechanical modes on. It turns out that in case of presented model this range is smaller than when the quantum contact models are concerned (here the models are based on the modulation doped structure [13]). It may stem from a different intensity of electric field distribution inside a device.

Acknowledgment

This work was supported by the State Committee for Scientific Research under grant No. 3-T11B-093-28.

References

1. M. A. Kastner, *The Single-Electron Transistor*, Rev. of Modern Phys., 1992,**64**, 3, 849–858.
2. J. L. Doob, *Classical Potential Theory and Its Probabilistic Counterpart*, Springer, New York, 1984.
3. S. Pawłowski, A. Kusy, R. Sikora, M. Mączka, E. Machowska-Podsiadło, *Numerical Studies of Quantum Dot Electrical Transport Properties*, in Metal/Non-Metal Microsystems: Physics, Technology and Applications, Licznerski B. W., Dziedzic A., Eds., Proc. SPIE 2780, 1995, 202–207.
4. E. N. Economou, *Green's Functions in Quantum Physics*, Springer, New York, 1983.
5. S. Datta, *Electronic Transport in Mesoscopic Systems*, Cambridge University Press, 1995.
6. J. H. Davies, *The Physics of Low-Dimensional Semiconductors*, Cambridge University Press, 1998.
7. R. Landauer, *Conductance from Transmission: Common Sense Points*, Phys. Scripta, 1992, **T42**, 110.
8. D. S. Fisher, P. A. Lee, *Relation between Conductivity and Transmition Matrix*, Phys. Rev. B, 1981, **23**, 6851.
9. M. J. McLennan, Y. Lee, S. Datta, *Voltage Drop in Mesoscopic Systems: A Numerical Study Using a Kinetic Equation*, Phys. Rev. B, 1991, **43**, 13846.
10. A. Kolek, G. Hałdaś, *Modelling of Quantum Mechanical Devices by Green's Function Technique*, Acta Phys. Pol. B, 2000, **32**, 551–556.
11. M. I. Reznikov, M. Heiblum, H. Shtrikman, D. Mahalu, *Temporal Correlation of Electrons: Suppression of Shot Noise in a Ballistic Quantum Point Contact*, Phys. Rev. Lett., 1995, **75**, 3340–3343.
12. B. J. van Wees, H. van Houten, C. W. J. Beenakker, J. G. Williamson, L. P. Kouwenhoven, D. van der Marel, C. T. Foxon, *Quantized Conductance of Point Contacts in a Two-Dimensional Electron Gas*, Phys. Rev. Lett., 1988, **60**, 848–850.
13. J. A. Nixon, J. H. Davies, H. U. Baranger, *Breakdown of Quantized Conductance in Point Contacts Calculated Using Realistic Potentials*, Phys. Rev. B, 1991, **43**, 12638–12641.